

Actual field corrosion rate of offshore structures in the Baltic Sea along depth profile from water surface to sea bed

Juliusz Orlikowski^{a)}, Michał Szociński^{a)*}, Krzysztof Żakowski^{a)}, Piotr Igliński^{b)}, Kinga Domańska^{b)}, Kazimierz Darowicki^{a)}

^aDepartment of Electrochemistry, Corrosion and Materials Engineering, Faculty of Chemistry, Gdańsk University of Technology, G. Narutowicza Str. 11/12, 80-233 Gdańsk, POLAND,

^b LOTOS Petrobaltic S.A., Stary Dwór Str. 9, 80-758 Gdańsk, POLAND

Abstract

The paper presents the results of field electrochemical investigations on the corrosion rate of carbon steel in seawater of the Baltic Sea at the location of the Baltic Beta production rig. The measurements were conducted throughout the year in seawater at different depths from the sea surface to the sea bed (about 75 m). The results revealed corrosion aggressiveness of the seawater along the entire depth profile. There was no multiple decrease in the corrosion rate of carbon steel at deeper levels (below 15 m), which had been observed in the literature reporting the investigations in the seas and oceans of higher salinity (3.5%) than southern Baltic Sea (about 0.8%). A model for monitoring water physico-chemical parameters along a depth profile showed the presence of a substantial amount of oxygen far below the sea surface, which translated into high corrosion aggressiveness of the Baltic seawater. Throughout the year corrosion rate is higher than 0.8 mm/year at the sea surface and even 0.4 mm/year at the sea bed. Presented results can constitute a guideline for the design of the anticorrosion protection systems for offshore wind farms or oil and gas production platforms in the Baltic Sea region.

28 **Keywords:** Baltic Sea; corrosion aggressiveness of water; offshore wind farms; offshore oil
29 production platforms; corrosion depth profile

30

31 **1. Introduction**

32 The Baltic Sea is a large water reservoir, the chemical composition of which differs
33 significantly from ocean water (Hakanson and Bryhn, 2008). Baltic seawater contains much
34 fewer inorganic salts due to poor water exchange with the North Sea via the narrow Danish
35 straits and due to a substantial inflow of sweet water from the surrounding rivers (Hakanson
36 and Bryhn, 2008). The Baltic Sea is a very convenient localization for wind farms, because of
37 the relatively low depths of the sea allowing building of the farms at distant offshore
38 locations, as well as oil and gas platforms (List of offshore wind farms in the Baltic Sea,
39 2022). This asset is confirmed by the onset of new energetic investments in the Baltic Sea
40 region. Building of the wind farms and oil production platforms requires suitable
41 anticorrosion protection, especially because of very limited possibilities for future
42 maintenance and repair (submerged zones). Applied anticorrosion protection technology
43 should be effective throughout most of the lifetime of hydrotechnical structures. To achieve
44 this goal, corrosion aggressiveness for the submerged structures must be precisely recognized
45 (Khodabux et al., 2020).

46 In general, corrosion rate in seawater depends on many factors: water temperature (an
47 increase in temperature is accompanied by higher kinetics of corrosion processes – corrosion
48 rate increases) (Porte, 1967), the content of inorganic salts in water (presence of more
49 corrosive zone depending on salt content) (Heldtberg et al., 2004), oxygen content in water
50 (lower oxygen content enhances diffusion control over corrosion process and corrosion rate
51 decreases) (Porte, 1967; Nevshupa et al., 2018), the erosive impact of water causing a local
52 increase in oxygenation and primarily the removal of the corrosion products which limit the



53 corrosion rate, presence of aerobic and anaerobic bacteria imposing an additional risk of
54 microbiological corrosion (Bale et al., 1997; Barnes et al., 1998; Dick et al., 2013). The
55 influence of solar radiation on the corrosion rate of cathodically protected carbon steel in
56 shallow seawater was investigated by Benedetti and co-workers (Benedetti et al., 2009). The
57 evaluation of the impact of particular water components on the corrosion rate is a very
58 difficult task and there are attempts to employ artificial neural networks to solve that problem
59 (Paul, 2012).

60 In principle, corrosion risk in seawater is divided into a few zones (American Bureau
61 of Shipping, 2018). The first one is a splash zone, in which the structure experiences
62 periodical contact with seawater. It is the region with the highest corrosion rate due to water
63 erosive impact on formed corrosion products (Refait et al., 2020). The next is a tidal zone
64 where corrosion risk is lower (periodical mechanical water impact on a structure). A
65 permanent immersion zone (water column zone) is characterized by the corrosion rate 5-times
66 lower than the splash zone. The deepest zones include a sea bed zone with a much lower
67 corrosion rate (oxygen deficit) and a marine sediment zone with the lowest corrosion rate
68 (Chen et al., 2020). The corrosion rate of carbon steel was evaluated in detail for the
69 aforementioned zones in the Atlantic Ocean (Yan et al., 2019). Corrosivity of particular zones
70 was also addressed regarding the application of protective coatings (Lopez-Ortega et al.,
71 2019; Det Norske Veritas AS, 2015). The literature provides data on a detailed analysis of
72 corrosion risk along the depth profile of the Atlantic Ocean, including significant depths
73 (Khodabux et al., 2020; Venkatesan et al., 2002; Imbert et al., 1999; Massi et al., 2019).
74 Haynes et al. revealed that in deep regions oxygen content in water was 3 ppm, which
75 suggests that corrosion with oxygen depolarization can still occur at high depths (Haynes,
76 1967). The investigations were also conducted in deep ocean regions, for instance in the
77 geothermal water release zone (Lavaleye et al., 2014).



78 The results of investigations on the corrosion rate of steel in seawater of the Baltic Sea
79 are available in the literature. Aromaa and Forsén carried out long-term exposure of the
80 corrosion coupons placed in the vicinity of the sea surface in the Gulf of Finland (Aromaa and
81 Forsen, 2016). Żakowski et al. reported very diversified water aggressiveness near the river
82 mouths due to big changes in salinity (Żakowski et al., 2014). Nevertheless, there is a lack of
83 information on the Baltic seawater corrosion aggressiveness at different depths of immersion
84 of the hydrotechnical structures, on a seasonal basis.

85 The aim of this paper is the evaluation of the corrosion rate of carbon steel based on
86 electrochemical measurements performed in the seawater at different depths from the sea
87 surface to the sea bed. The results of the investigations will facilitate the proper design of the
88 anticorrosion protection systems for offshore wind farms or oil and gas platforms in the Baltic
89 Sea region.

90

91 **2. Material and methods**

92 A comparative analysis employed the data from an eco-hydrodynamic numerical
93 model (Ołdakowski et al., 2005; Jędrasik and Kowalewski, 2019). The ProDeMo (Production
94 and Destruction of Organic Matter Model), a 3D coupled hydrodynamic-ecological model,
95 was elaborated and applied to the whole Baltic Sea and the subregion of the Gulf of Gdansk.
96 The model generates numerous data related to the physical, chemical, and biological
97 composition of water from the entire area of the Baltic Sea. More importantly, the model also
98 provides seawater parameters along a depth profile, which is valuable information allowing
99 verification of the results of electrochemical measurements. The model consists of two
100 modules – hydrodynamic M3D_UG and ecosystem ProDeMo ones. It works in a pre-
101 operational mode over the southern Baltic Sea, Gdansk Bay, and Pomeranian Bay. 60-hour
102 forecasts engulf surface currents, temperature, and seawater salinity. Moreover, the prognoses
103 concern biogenic salts, including nitrates, ammonia, phosphates, and silicates, as well as total



104 nitrogen and phosphorus, oxygen concentration in seawater and biomass of phytoplankton.
105 The results of prognoses are archived and they were taken advantage of in this paper. The
106 eco-hydrodynamic model is verified with the data on seawater level, temperature, and salinity,
107 which are received from the measurement stations (the buoys) distributed in various places
108 over the Baltic Sea. The investigations presented in this paper were carried out at the location
109 of one of these measurement-verification stations, which ensures relatively low error in
110 conducted studies. Archive and prognosis data from the model are available at
111 <http://model.ocean.univ.gda.pl/php/frame.php?area=Baltyk>.

112 The electrochemical measurements were conducted with an electrochemical
113 workstation Gamry Reference 600. The following tests were carried out:

- 114 • Linear Polarization Resistance (LPR) measurements – analysis of the corrosion rate
115 of carbon steel. Potentiodynamic measurement was performed for the following
116 parameters: potential scan rate 0.125 mV/s, polarization range ± 20 mV with respect to
117 OCP (open circuit potential),
- 118 • Measurement of Tafel curves – analysis of Tafel coefficients regarding changes of the
119 control over corrosion processes depending on oxygen content in water.
120 Potentiodynamic measurement was performed for the following parameters: potential
121 scan rate 1 mV/s, polarization range ± 250 mV with respect to OCP,
- 122 • Electrochemical Impedance Spectroscopy (EIS) measurements – analysis of the
123 electrolyte resistance changes regarding the variation of water salinity. The
124 measurement frequency range was from 5 Hz to 0.01 Hz and the amplitude of ac
125 perturbation signal was 10 mV.

126
127 The measurements were conducted using a dedicated three-electrode sensor (the
128 working, reference and auxiliary electrode, each of them made of S235JR steel, the surface



129 area of each electrode was 0.5 cm^2) submerged on a long cable from a deck of the Baltic Beta
130 platform. The sensor was gradually dropped towards the sea bed (75 m) with periodical stops
131 for the execution of the measurements at precisely determined depths. The production rig was
132 located 60 km offshore at the Baltic Sea with the following geographical coordinates (55
133 28.82°N ; $18^{\circ}10.77^{\circ}\text{E}$). On this production rig, the modernized cathodic protection system has
134 been in continuous operation since 2009 (Żakowski et al., 2020).

135 Fig. 1 illustrates the measurement location and position. The selection of the
136 measurement cable ensured the limitation of its resistance (cross-section 2.5 mm^2) and
137 minimization of interferences (shielded insulation).

138

139

140

141

142

143

144

145

146

147

148

149

150

151

152

153



154 a)

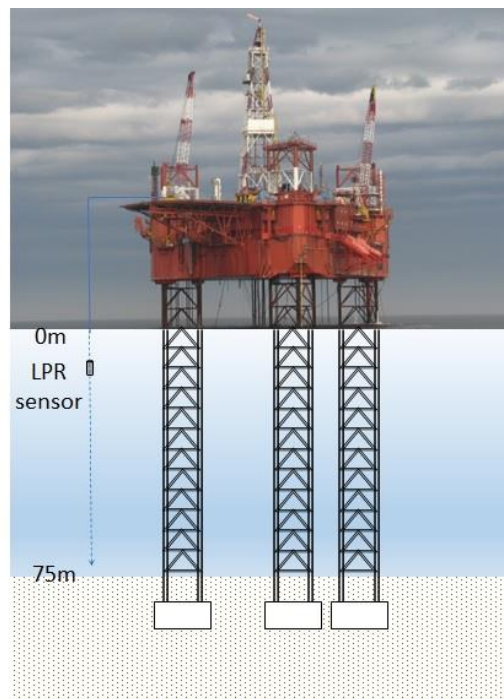


b)



155

156 c)



157

158

159 Fig. 1. The measurement location (a), position (b), and scheme of sensor orientation with
160 respect to the Baltic Beta production rig.

161

162 The field measurements were preceded by a series of laboratory measurements in
163 seawater aimed at evaluating the influence of the long cable (100 m) on the measurement
164 error. They revealed no significant measurement error in the case of the LPR and Tafel curves
165 techniques (less than 2%). For EIS, the error higher than 10% was identified in the frequency

166 range above 10 kHz. That is why it was decided to execute the impedance measurements
167 between 10 kHz and 0.01 Hz.

168 The field measurements were conducted on three dates throughout the year to evaluate
169 the corrosion rate of carbon steel along a depth profile depending on water temperature and its
170 seasonal chemical composition. The measurement dates were as follows:

- 171 • 22.11.2020 – autumn and spring conditions,
- 172 • 19.04.2021 – winter conditions,
- 173 • 3.07.2021 – summer conditions.

174 These measurement dates do not fully correspond to the calendar seasons of the year,
175 which results from a delayed reaction of seawater temperature to seasonal changes in air
176 temperature. The selection of the measurement dates was based on data from the eco-
177 hydrodynamic model (Ołdakowski et al., 2005; Jędrasik and Kowalewski, 2019).

178 The measurements were carried out at depth intervals of 10-15 m starting from the sea
179 surface down to the sea bed at 75 m.

180 The investigation also involved corrosion rate measurement with a gravimetric method
181 employing corrosion coupons. 3 coupons were mounted to the steel structure of the
182 production rig at the depth of 0.5 m below the sea surface. The coupons were made of S235JR
183 steel, which is the construction material of the Baltic Beta production rig. They were in the
184 form of plates having the following dimensions: 35 cm x 10 cm x 0.2 cm (thickness). Before
185 exposure, the coupons were ground with abrasive paper of 120 gradation and degreased with
186 acetone.

187
188
189
190



191 **3. Results and discussion**

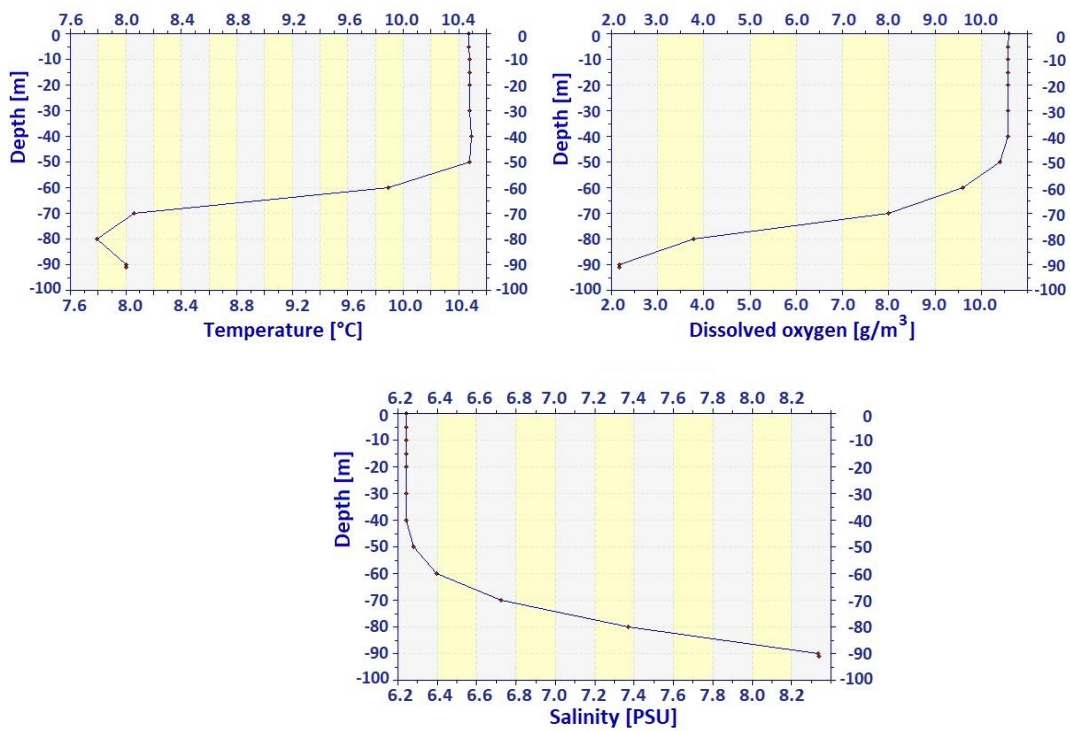
192 **3.1 Physical properties of the Baltic seawater**

193 Fig. 2 presents basic data on the physical properties of the seawater based on the data
194 from the eco-hydrodynamic model.

195

196 a)

197



198

199

200

201

202

203

204

205

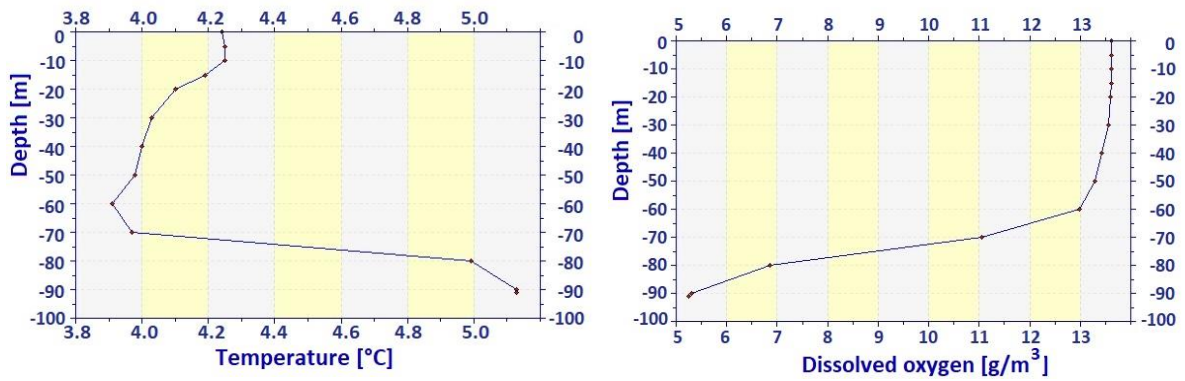
206

207

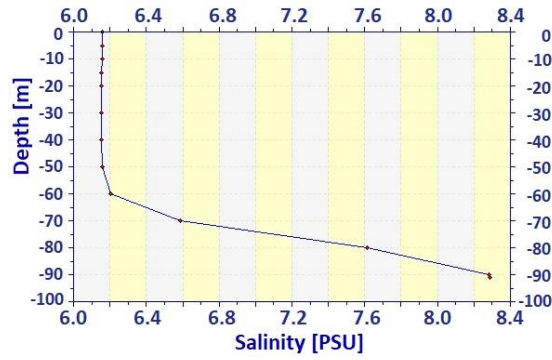
208

209

210 b)



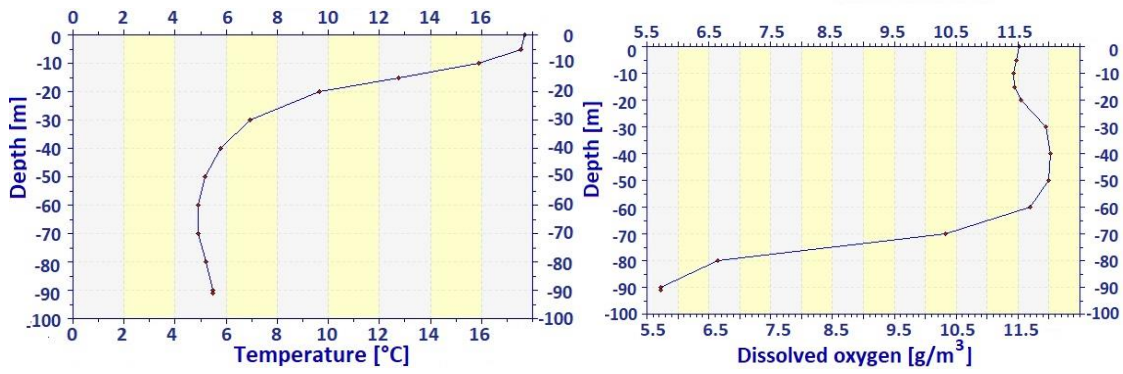
211



212

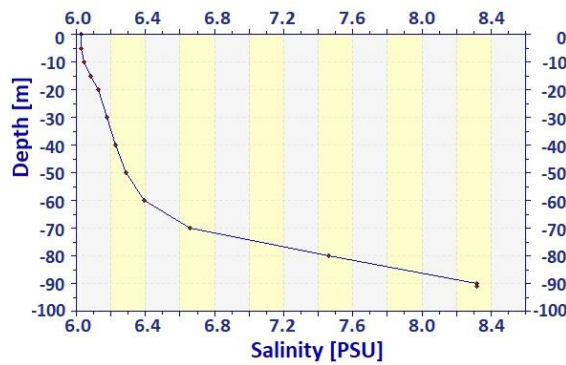
213

214 c)



215

216



217

218 Fig. 2. Data on temperature, salinity, and oxygen content in water based on the eco-
219 hydrodynamic model: (a) 22.11.2020, (b) 19.04.2021, (c) 03.07.2021.

220

221 Presented data from the model engulf temperature, salinity, and oxygen content in
222 water along a depth profile from the sea surface to the sea bed. It must be emphasized that the
223 model data do not necessarily overlap with the actual data, nevertheless, they can be the basis
224 for evaluation of corrosion aggressiveness of water. The data show that seawater in the Baltic
225 Sea is characterized by relatively high oxygen content along a wide range of the depth profile,
226 which indicates no significant diffusion limitations of the corrosion rate due to oxygen deficit.
227 Results of the measurements reveal that oxygen deficit can occur only in autumn. This
228 phenomenon is connected with hypoxia, which is a seasonal oxygen deficit near the sea bed
229 of the Baltic Sea that has practically occurred since prehistoric times (Conley et al., 2009;
230 Zillen et al., 2008). The main factors responsible for this effect are the meteorological
231 conditions connected with wind direction and speed, which pushes oxygenated and more
232 saline water from the North Sea towards the Baltic Sea. This water of higher specific gravity
233 migrates to the regions close to the sea bed (higher salinity visible in Fig. 2). Initially it
234 contains a significant amount of oxygen, however, during the periods of poor or no water
235 exchange between the North Sea and the Baltic Sea there is oxygen depletion due to the
236 biological processes. Horizontal exchange with sweet water is limited as a halocline occurs.
237 Due to this barrier, there is the seasonal formation of a low-oxygen water layer in the vicinity
238 of the sea bed, especially in deeper regions of the Baltic Sea (Conley et al., 2002).

239 An increase in salinity near the sea bed is not high, which suggests that it may not
240 have a substantial impact on oxygen content and the corrosion rate of carbon steel. The
241 investigations show a high water temperature gradient during the summertime, which can
242 influence changes in corrosion rate along the depth profile.

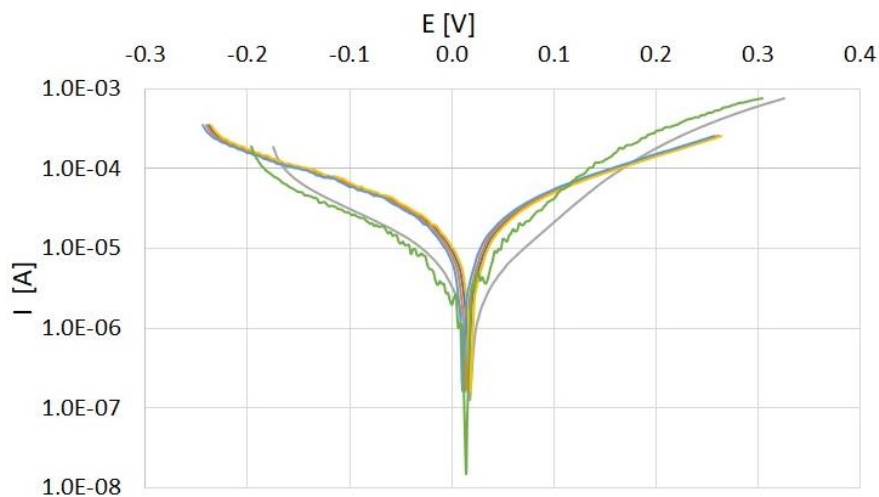


243 **3.2 Results of electrochemical investigations**

244 Fig. 3 presents the Tafel curves obtained during the electrochemical measurements
245 conducted in the Baltic Sea at the platform location.

246

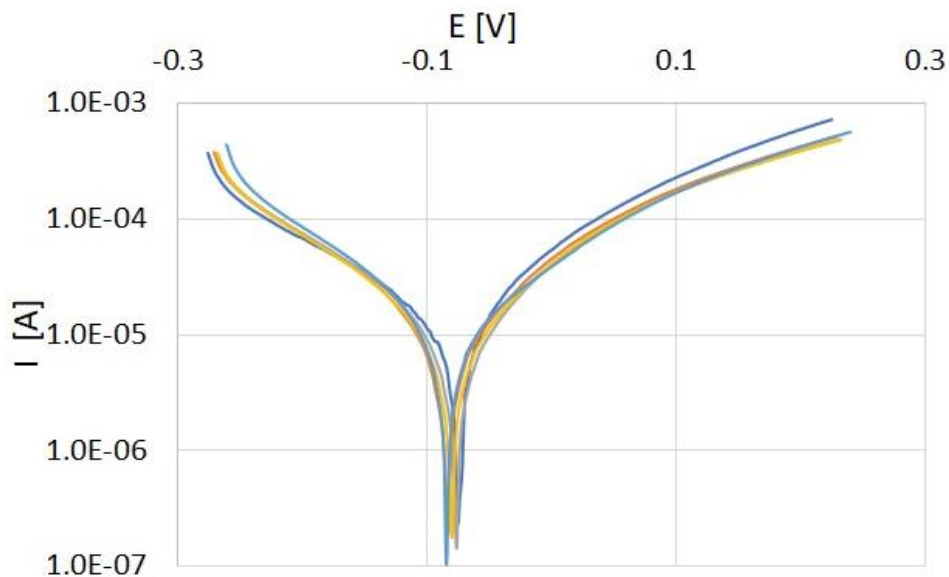
247 a)



248

249

250 b)



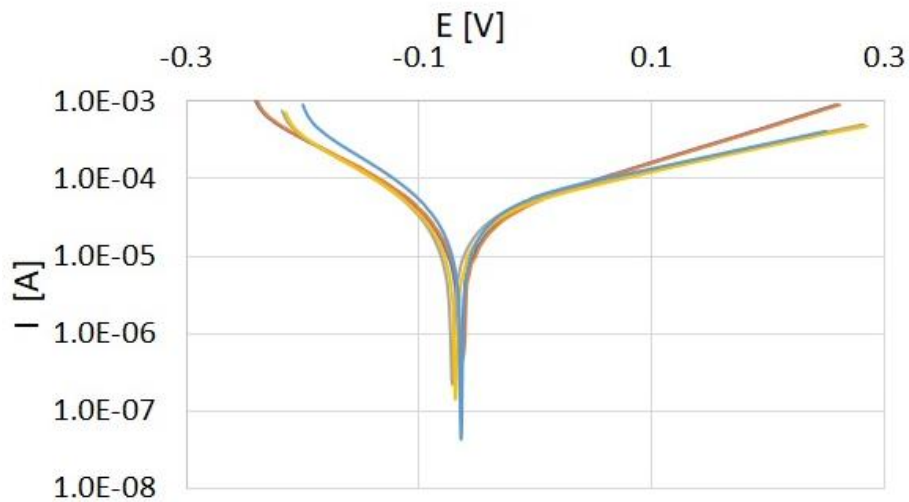
251

252

253

254

255 c)



256

257 Fig. 3. Results of Tafel curves measurement along a depth profile: a) 22.11.2020, b)

258 19.04.2021, c) 3.07.2021. Depths: light blue – 0 m, dark blue – 15 m, orange – 30 m, yellow –

259 50 m, grey – 60 m, green – 75 m.

260

261 There is a high similarity in the courses of the potentiodynamic plots, indicating a
 262 similar corrosion rate of carbon steel along the entire depth profile. Significant differences
 263 occur only in the case of the measurements at 60 and 75 m, conducted in autumn. The results
 264 of a more detailed analysis of the Tafel curves are gathered in Tab. 1.

265

266 Tab. 1. Values of Tafel coefficients and corrosion rate calculated based on potentiodynamic
 267 measurements.

Depth [m]	22.11.2020			19.04.2021			03.07.2021		
	b_a [V]	b_k [V]	Vcorr [mm/y]	b_a [V]	b_k [V]	Vcorr [mm/y]	b_a [V]	b_k [V]	Vcorr [mm/y]
0	0.286	0.316	0.753	0.216	0.334	0.732	0.221	0.134	0.950
15	0.283	0.286	0.630	0.229	0.251	0.702	0.283	0.13	0.832
30	0.208	0.255	0.603	0.227	0.221	0.651	0.308	0.132	0.878
50	0.156	0.336	0.605	0.228	0.237	0.634	0.310	0.134	0.786
60	0.131	0.239	0.421	0.195	0.193	0.571	0.315	0.120	0.750
75	0.118	0.142	0.241	0.187	0.165	0.532	0.317	0.117	0.701

268 The Tafel coefficients exhibit high coherence for particular depth profiles, which
 269 means that the corrosion mechanism is similar in each case. One can notice differences in the
 270 measurements near the sea bed, especially on 22.11.2020, where a decrease in the Tafel
 271 coefficients is recorded, which can be evidence of a decreased level of oxygen in the water.
 272 Tab. 2 presents the values of electrolyte resistance determined based on EIS measurements
 273 (Narożny et al., 2017). This parameter provides information related to the content of various
 274 salts in water. The lower the electrolyte resistance, the higher concentration of salts in water.
 275 This dependence also holds for water resistivity changes upon different salt content. Thus,
 276 these two parameters are correlated as far as seawater salinity investigation is concerned.

277

278 Tab. 2. Electrolyte resistance along a depth profile determined via EIS measurements.

	22.11.2020	19.04.2021	03.07.2021
Depth [m]	Electrolyte resistance [Ω]		
0	75	94	70
15	105	109	94
30	104	109	103
50	78	109	109
60	75	109	109
75	69	77	77

279

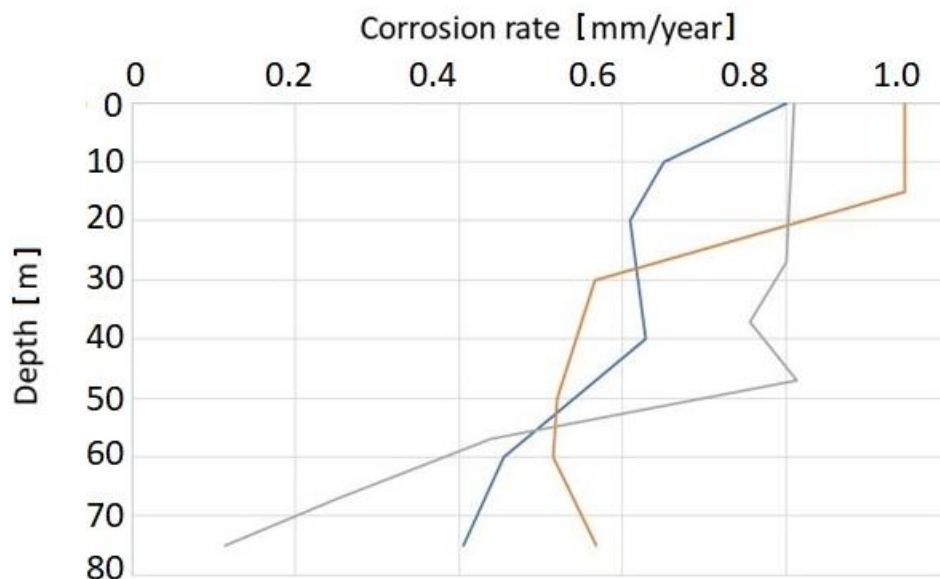
280 The magnitude of electrolyte resistance can be associated with water salinity level and
 281 the presence of other factors contributing to an increase in water conductivity. The
 282 investigations (Tab. 2) revealed a decrease in electrolyte resistance near the sea surface and
 283 sea bed. The decrease in resistance in the vicinity of the sea bed is in accordance with the
 284 results from the eco-hydrodynamic model, which predicts an increase in seawater salinity.
 285 The reasons for low electrolyte resistance in the surface zone remain unknown.

286 Fig. 4 depicts the corrosion rate of carbon steel obtained using the LPR method.

287

288





289

290 Fig. 4. Corrosion rate of carbon steel along a depth profile determined via LPR

291 measurements: grey – 22.11.2020, blue 19.04.2021, orange – 19.07.2021.

292

293 The results show that the corrosion rate of carbon steel in the Baltic Sea is high and
 294 generally consistent with the data from the eco-hydrodynamic model. The highest corrosion
 295 rate (which is in accordance with the literature data) occurs at the sea surface and is equal to
 296 about 0.8-0.9 mm/year and then decreases to only 30% of the surface value in the tidal zone,
 297 which is a different result as compared to corrosion rate measurements in the other water
 298 reservoirs (Yan et al., 2019). As suggested in scientific literature, the corrosion rate values for
 299 carbon steel in a permanent immersion zone amount to 0.20-0.35 mm/year (Yan et al., 2019).
 300 A significant decrease in corrosion rate near the sea bed was identified only in autumn. The
 301 values of corrosion rate acquired via the LPR method are in high agreement with the ones
 302 determined based on the Tafel curves.

303

304 3.3 Results of corrosion rate investigations with coupon method

305 Presented results were verified with the gravimetric method employing corrosion
 306 coupons and non-destructive ultrasonic wall thickness measurements. Fig. 5a presents an

307 underwater coupon exposure system, which was mounted to the steel structure of the
308 production rig at the depth of 0.5 m below the sea surface. The condition of an exemplary
309 corrosion coupon after 6-month exposure is depicted in Fig. 5b and Fig. 5c.

310

311 a)



312

313 b)



c)



314

315

316 Fig. 5. Underwater coupon exposure system mounted to production rig (a), condition of
317 exemplary corrosion coupon after 6-month exposure: before cleaning (b) and after removal of
318 corrosion products and biological deposits (c).

319

320 The exposure involved 3 corrosion coupons located directly below sea level, in the
321 immersion zone. After retrieving, an inspection of the coupons revealed the presence of

322 biological deposits (diatoms) and corrosion products on their surface (Fig. 5). In order to
323 determine the corrosion rate, the coupons were cleaned and their mass was measured. Tab. 3
324 shows the corrosion rate of the coupons exposed in the immersion zone of the production rig.

325

326 Tab. 3. Corrosion rate of coupons exposed in immersion zone of the Baltic Beta production
327 rig.

Coupon no.	Corrosion rate [mm/year]
1	0.376
2	0.335
3	0.356

328

329 The corrosion rate determined using the gravimetric measurements is lower than the
330 one obtained with the LPR investigations. The reason is the inhibitive action of the organic
331 deposits and corrosion products.

332

333 **3.4 Results of non-destructive tests**

334 Additionally, non-destructive ultrasonic wall thickness measurements were carried out
335 on the submerged structure of the production rig. An exemplary report from such tests is
336 presented in Tab. 4.

337

338

339

340

341

342

343

344 Tab. 4. Exemplary report from ultrasonic wall thickness measurements performed in
 345 immersion zone on the steel structure of the Baltic Beta production rig.

Ship's name: BALTIC BETA Class Identity No. 680112 Report No. 38/16				
Structural member: CHORD No. 1 – BRACINGS CONNECTION				
Location of structure: LEG No. 1; BAY 15				
Description	Org. Thx. [mm]	Gauged [mm]	Diminution	
			[mm]	[%]
Vert. diagonal bracing VD1 plating:				
section D (casting) – read. 1	19.0	16.4	2.6	13.7
section D (casting) – read. 2	19.0	16.5	2.5	13.2
section D (casting) – read. 3	19.0	17.5	1.5	7.9
section D (casting) – read. 4	19.0	17.4	1.6	8.4
section E – read. 1	19.05	15.0	4.1	21.3
section E – read. 2	19.05	15.3	3.8	19.7
section E – read. 3	19.05	16.4	2.7	13.9
section E – read. 4	19.05	16.7	2.4	12.3
section F – read. 1	19.05	14.6	4.5	23.4
section F – read. 2	19.05	16.9	2.2	11.3
section F – read. 3	19.05	17.5	1.6	8.1
section F – read. 4	19.05	18.5	0.6	2.9
section G – read. 1	19.05	15.9	3.2	16.5
section G – read. 2	19.05	17.1	2.0	10.2
section G – read. 3	19.05	18.0	1.1	5.5
section G – read. 4	19.05	17.9	1.2	6.0

346
 347 The investigations revealed the maximum corrosion loss of ca. 4.5 mm during 20
 348 years of exposure. The corrosion rate was equal to 0.225 mm/year. During the initial exposure
 349 period, the corrosion rate was impeded by the presence of organic protective coatings applied
 350 on the legs of the production rig.

351
 352 The novelty of the work, with respect to other data and papers available, is different
 353 from the expected corrosion risk of hydrotechnical structures. In most cases, the corrosion rate
 354 is believed to decrease significantly below the splash zone due to lower oxygen content in
 355 water. Moreover, oxygen is believed to be practically absent in water in deep regions. These

356 observations are the basis for the design of anticorrosion protection for hydrotechnical
357 structures. For instance, no organic coatings and significantly simplified cathodic protection
358 systems are accepted in Baltic seawater at depths exceeding 15 m. The results of conducted
359 studies indicate that the limitation of the anticorrosion protection measures in deep regions
360 may be an incorrect approach in this case. Implementation of experience and experimental
361 results acquired from other oceans and seas (with completely different chemical
362 compositions) is not entirely correct. The uniqueness and novelty of performed investigations
363 are also connected with the fact that the measurements were carried out on a real
364 hydrotechnical structure, which is located at high depths of the Baltic Sea. Most of the
365 literature data available so far originate from the measurement stations at the seashore. The
366 presented findings can be key data for the design of anticorrosion protection of offshore wind
367 farms, which soon are going to be built in the Baltic Sea.

368 The investigations have been conducted at one location in the Baltic Sea. Despite the
369 evident correlation between corrosion rate and physico-chemical properties of seawater, one
370 cannot exclude local deviations from the obtained results, especially during stormy weather.

371

372 **4. Conclusions**

373 The performed field investigations involved electrochemical, gravimetric, and non-
374 destructive measurements to determine the corrosion rate of carbon steel in seawater of the
375 Baltic Sea at the location of the Baltic Beta production rig. The obtained data were discussed
376 with respect to the physico-chemical parameters of the Baltic seawater collected within the
377 frame of the eco-hydrodynamic model. Accordingly, the following conclusions can be drawn:

- 378 – The investigations revealed that the corrosion rate of carbon steel in the Baltic
379 seawater along the depth profile differed significantly from the corrosion rate in the
380 water reservoirs of higher salinity and located in other climatic zones. Contrary to
381 them, in the Baltic Sea, no multiple decrease in the corrosion rate of carbon steel was



382 noticed along the water column due to high oxygen content, confirmed by the data
383 from the eco-hydrodynamic model. For most time throughout the year, the corrosion
384 rate is higher than 0.8 mm/year at the sea surface and 0.4 mm/year at the Baltic Sea
385 bed.

- 386 – Analysis of the Tafel coefficients indicates no distinct changes in the corrosion
387 mechanism at each depth. At every investigated level the corrosion process occurs
388 with oxygen depolarization as a cathodic reaction.
- 389 – Differences in water salinity at various depths of the Baltic Sea are not big, which
390 does not translate into a significant reduction in the corrosion rate in the sea bed zone.
- 391 – It was found that oxygen content decreases near the sea bed only in a seasonal way,
392 which limits the corrosion rate at the sea bed from about 0.4 mm/year to 0.2 mm/year.
- 393 – From the obtained results it follows that in the future design of the hydrotechnical
394 structures intended for submersion in the Baltic Sea, the anticorrosion protection
395 technology (cathodic protection, protective coatings) should be selected in the way,
396 which takes substantial corrosion risk along the entire depth profile into account.

397 In general, future work will focus on the analysis of the corrosion rate acquired from the
398 coupon investigations, which are currently being conducted along the entire depth profile.
399 Moreover, the emphasis will be put on changes in the corrosion rate in the vicinity of a sea bed
400 due to significant fluctuations of oxygen content in water. Accordingly, the investigations will
401 be carried out at higher depths as well as below the sea bed.

402
403
404
405
406
407



408 **References**

409 American Bureau of Shipping, 2018. ABS – 306: Guidance Notes On Cathodic Protection Of
410 Offshore Structures, Spring, Texas.

411 Aroma, J., Forsen, O., 2016. Factors affecting corrosion in Gulf of Finland brackish water.
412 Int. J. Electrochem. Sci. article ID 3720280. <http://dx.doi.org/10.1155/2016/3720280>.

413 Bale, S.J., Goodman, K., Rochelle, P.A., Marchesi, J.R., Fry, J.C., Weightman, A.J., Parkes,
414 R.J., 1997. *Desulfovibrio profundus* sp. nov., a novel barophilic sulfate-reducing bacterium
415 from deep sediment layers in the Japan Sea. Int. J. Syst. Evol. Microbiol. 47, 515–521.
416 <https://doi.org/10.1099/00207713-47-2-515>.

417 Barnes, S.P., Bradbrook, S.D., Cragg, B.A., Marchesi, J.R., Weightman, A.J., Fry, J.C.,
418 Parkes, R.J., 1998. Isolation of sulfate-reducing bacteria from deep sediment layers of the
419 pacific ocean. Geomicrobiol. J. 15, 67-83. <https://doi.org/10.1080/01490459809378066>.

420 Benedetti, A., Magagnin, L., Passaretti, F., Chelossi, E., Faimali, M., Montesperelli, G., 2009.
421 Cathodic protection of carbon steel in natural seawater: effect of sunlight radiation.
422 Electrochim. Acta. 54, 6472–6478. doi:10.1016/j.electacta.2009.06.022.

423 Chen, Z., Xia, W., Yao, C., Lin, Z., Zhang, W., Li, W., 2020. Research on the metal corrosion
424 process in the sea mud/seawater/atmosphere interface zone. Coatings. 10, 1219.
425 doi:10.3390/coatings10121219.

426 Conley, D.J., Humborg, C., Rahm, L., Savchuk, O.P., Wulff, F., 2002. Hypoxia in the Baltic
427 Sea and basin-scale changes in phosphorus biogeochemistry. Environ. Sci. Technol. 36, 5315-
428 5320. <https://doi.org/10.1021/es025763w>.

429 Conley, D.J., Bjorck, S., Bonsdorff, E., Carstensen, J., Destouni, G., Gustafsson, B.G.,
430 Hietanen, S., Kortekaas, M., Kousa, H., Markus Meier, H.E., Muller-Karulis, B., Nordberg,
431 K., Norkko, A., Nurnberg, G., Pitkanen, H., Rabalais, N.N., Rosenberg, R., Savchuk, O.P.,



432 Slomp, C.P., Voss, M., Wulff, F., Zillen, L., 2009. Hypoxia-related processes in the Baltic
433 Sea. *Environ. Sci. Technol.* 43, 3412-3420. <https://doi.org/10.1021/es802762a>.

434 Det Norske Veritas AS, 2015. Recommended Practice DNVGL-RP-C302 Risk Based
435 Corrosion Management.

436 Dick, G.J., Anantharaman, K., Baker, B.J., Li, M., Reed, D.C., Sheik, C.S., 2013. The
437 microbiology of deep-sea hydrothermal vent plumes: ecological and biogeographic linkages
438 to seafloor and water column habitats. *Front. Microbiol.* 4, article 124.
439 <https://doi.org/10.3389/fmicb.2013.00124>.

440 Hakanson, L., Bryhn, A.C., 2008. *Eutrophication in the Baltic Sea*, Springer, Berlin,
441 Heidelberg.

442 Haynes, W.S., Outline of an approach to a long range research, development and evaluation
443 program on prevention of deterioration of materials of construction, as an appendix in Porte,
444 H.A., 1967. *The Effect of Environment on the Corrosion of Metals in Sea Water – A*
445 *Literature Survey*, U.S. Naval Civil Engineering Laboratory, Port Hueneme, California.

446 Heldtberg, M., MacLeod, I.D., Richards, V.L., 2004. Corrosion and cathodic protection of
447 iron in seawater: a case study of the James Matthews (1841). *Proceedings of Metal 2004*.
448 National Museum of Australia Canberra ACT. 75-87.

449 Imbert, C.A.C., Ragoonath, D., Lewis, W.G., 1999. Corrosion of offshore platforms off the
450 south-east coast of Trinidad. *WIJE.* 21, 1-8.

451 Jędrasik, J., Kowalewski, M., 2019. Mean annual and seasonal circulation patterns and long-
452 term variability of currents in the Baltic Sea. *J. Mar. Syst.* 193, 1-26.
453 <https://doi.org/10.1016/j.jmarsys.2018.12.011>.

454 Khodabux, W., Causon, P., Brennan, F., 2020. Profiling corrosion rates for offshore wind
455 turbines with depth in the North Sea. *Energies.* 13, 2518. doi:10.3390/en13102518.



456 Lavaleye, M., Morales, F.L., Duineveld, G., Verichev, S., de Jong, A., Boomsma, W., Smit,
457 M., 2014. Study of deep sea corrosion near hydrothermal vents. Deployment of 5 x 37
458 construction materials for in-situ long-term exposure. Report from MIIP Project: Deep Corr
459 On Site, Nederland Maritiem Land.

460 List of offshore wind farms in the Baltic Sea.
461 https://en.wikipedia.org/wiki/List_of_offshore_wind_farms_in_the_Baltic_Sea (accessed 26
462 April 2022).

463 Lopez-Ortega, A., Bayon, R., Arana, J.L., 2019. Evaluation of protective coatings for high-
464 corrosivity category atmospheres in offshore applications. *Materials*. 12, 1325.
465 doi:10.3390/ma12081325.

466 Masi, G., Matteucci, F., Tacq, J., Balbo, A., 2019. State of the Art Study on Materials and
467 Solutions against Corrosion in Offshore Structures, NeSSIE - North Sea Solutions for
468 Innovation in Corrosion for Energy.

469 Narożny, M., Żakowski, K., Darowicki, K., 2017. Time evolution of electrochemical
470 impedance spectra of cathodically protected steel in artificial seawater. *Constr. Build. Mater.*
471 154, 88–94. doi: 10.1016/j.conbuildmat.2017.07.191.

472 Nevshupa, R., Martinez, I., Ramos, S., Arredondo, A., 2018. The effect of environmental
473 variables on early corrosion of high–strength low–alloy mooring steel immersed in seawater.
474 *Mar. Struct.* 60, 226-240. <https://doi.org/10.1016/j.marstruc.2018.04.003>.

475 Ołdakowski, B., Kowalewski, M., Jedrasik, J., Szymelfenig, M., 2005. Ecohydrodynamic
476 model of the Baltic Sea. Part 1. Description of the ProDeMo model. *Oceanologia*. 47, 477-
477 516.

478 Paul, S., 2012. Modeling to study the effect of environmental parameters on corrosion of mild
479 steel in seawater using neural network. *Int. Sch. Res. Notices*. article ID 487351.
480 <https://doi.org/10.5402/2012/487351>.



481 Porte, H.A., 1967. The Effect of Environment on the Corrosion of Metals in Sea Water – A
482 Literature Survey, U.S. Naval Civil Engineering Laboratory, Port Hueneme, California.
483 Refait, P., Grolleau, A-M., Jeannin, M. , Remazeilles, C., Sabot, R., 2020. Corrosion of
484 carbon steel in marine environments: role of the corrosion product layer. *Corros. Mater.*
485 *Degrad.* 1, 198–218. doi:10.3390/cmd1010010.
486 Venkatesan, R., Venkataswamy, M.A., Bhaskaran, T.A., Dwarakadasa, E.S., Ravindran, M.,
487 2002. Corrosion of ferrous alloys in deep sea environments. *Br. Corros. J.* 37, 257-266.
488 doi:10.1179/000705902225006633.
489 Yan, X., Wang, Y., Du, Q., Jiang, W., Shang, F., Li, R., 2019. Research progress on factors
490 affecting oxygen corrosion and countermeasures in oilfield development. *E3S Web Conf.*
491 131, 01031. <https://doi.org/10.1051/e3sconf/201913101031>.
492 Żakowski, K., Narożny, M., Szociński, M., Darowicki, K., 2014. Influence of water salinity
493 on corrosion risk - the case of the southern Baltic Sea coast. *Environ. Monit. Assess.* 186,
494 4871-4879. <https://doi.org/10.1007/s10661-014-3744-3>.
495 Żakowski, K., Iglinski, P., Orlikowski, J., Darowicki, K., Domanska, K., 2020. Modernized
496 cathodic protection system for legs of the production rig – Evaluation during ten years of
497 service. *Ocean Eng.* 218, 108074. <https://doi.org/10.1016/j.oceaneng.2020.108074>.
498 Zillen, L., Conley, D.J., Andren, T., Andren, E., Bjorck, S., 2008. Past occurrences of hypoxia
499 in the Baltic Sea and the role of climate variability, environmental change and human impact.
500 *Earth Sci. Rev.* 91, 77-92. <https://doi:10.1016/j.earscirev.2008.10.001>.

501

502

503

504

505



506 **Funding**

507 This research did not receive any specific grant from funding agencies in the public,
508 commercial, or not-for-profit sectors.

509

510

511

512

513

514

515

516

517

518

519

520

521

522

523

524

525

526

527

528

529

530

531 **Figure captions**

532 Fig. 1. The measurement location (a), position (b), and scheme of sensor orientation with
533 respect to the Baltic Beta production rig.

534 Fig. 2. Data on temperature, salinity, and oxygen content in water based on the eco-
535 hydrodynamic model: (a) 22.11.2020, (b) 19.04.2021, (c) 03.07.2021.

536 Fig. 3. Results of Tafel curves measurement along a depth profile: a) 22.11.2020, b)
537 19.04.2021, c) 3.07.2021. Depths: light blue – 0 m, dark blue – 15 m, orange – 30 m, yellow –
538 50 m, grey – 60 m, green – 75 m.

539 Fig. 4. Corrosion rate of carbon steel along a depth profile determined via LPR
540 measurements: grey – 22.11.2020, blue 19.04.2021, orange – 19.07.2021.

541 Fig. 5. Underwater coupon exposure system mounted to production rig (a), condition of
542 exemplary corrosion coupon after 6-month exposure: before cleaning (b) and after removal of
543 corrosion products and biological deposits (c).

544

545

546

547

548

549

550

551

552

553

554

555



556 **Table captions**

557 Tab. 1. Values of Tafel coefficients and corrosion rate calculated based on potentiodynamic
558 measurements.

559 Tab. 2. Electrolyte resistance along a depth profile determined via EIS measurements.

560 Tab. 3. Corrosion rate of coupons exposed in immersion zone of the Baltic Beta production
561 rig.

562 Tab. 4. Exemplary report from ultrasonic wall thickness measurements performed in
563 immersion zone on the steel structure of the Baltic Beta production rig.